

Pressure-Induced Transformations and Optical Properties of the Two-Dimensional Tetragonal Polymer of C₆₀ at Pressures up to 30 GPa[¶]

K. P. Meletov^{a,*}, J. Arvanitidis^b, S. Assimopoulos^b, G. A. Kourouklis^b, B. Sundqvist^c

^aInstitute of Solid State Physics, Russian Academy of Sciences, Chernogolovka, Moscow oblast, 142432 Russia

^bPhysics Division, School of Technology, Aristotle University of Thessaloniki GR-540 06, Thessaloniki, Greece

^cDepartment of Physics, Umea University S-901 87, Umea, Sweden

*e-mail: mele@issp.ac.ru

Received April 24, 2002

Abstract—The Raman spectra of the two-dimensional tetragonal (2D(T)) polymeric phase of C₆₀ have been studied *in situ* at pressures up to 30 GPa and room temperature. The pressure behavior of the phonon modes shows an irreversible transformation of the material near 20 GPa into a new phase, most probably associated with the covalent bonding between the 2D polymeric sheets. The Raman spectrum of the high-pressure phase is intense and well resolved, and the majority of modes are related to the fullerene molecular cage. The sample recovered at ambient conditions is in a metastable phase and transforms violently under laser irradiation: the transformed material contains mainly dimers and monomers of C₆₀ and small inclusions of the diamond-like carbon phase. The photoluminescence spectra of the 2D(T) polymer of C₆₀ were measured at room temperature and pressure up to 4 GPa. The intensity distribution and the pressure-induced shift of the photoluminescence spectrum drastically differ from those of the C₆₀ monomer. The deformation potential and the Grüneisen parameters of the 2D(T) polymeric phase of C₆₀ have been determined and compared with those of the pristine material. © 2002 MAIK “Nauka/Interperiodica”.

1. INTRODUCTION

The polymeric forms of C₆₀ have attracted considerable attention because of their interesting structure and properties [1]. Pristine C₆₀ has a great potential for polymerization because of the existence of 30 double C=C bonds in the fullerene molecular cage. C₆₀ has been found to polymerize under illumination with visible and ultraviolet light [2] and upon alkali metal doping [3, 4]. The treatment of C₆₀ under various high-pressure and high-temperature conditions also leads to polymerization of the material (HPHT polymers) [5]. The covalent polymeric bonds are usually formed by the so-called [2 + 2] cycloaddition reaction via the formation of four-membered rings between adjacent fullerene molecules, resulting in an appreciable decrease in the intermolecular distance [2].

The structure and the dimensionality of HPHT polymers strongly depend on the pressure (*P*) and temperature (*T*) treatment conditions. The C₆₀ molecules form linear polymeric chains (one-dimensional polymer) having an orthorhombic crystal structure (1D(O)) and/or dimers and higher oligomers at lower *P* and *T*, two-dimensional polymeric layers that have either a rhombohedral (2D(R)) or a tetragonal (2D(T)) crystal structure at intermediate *P* and *T*, and face-centered

cubic structures based on three-dimensional (3D) cross-linked polymerization of the material at higher *P* and *T* [1, 5–7]. In addition, the treatment of the pristine material under high nonuniform pressure and high temperature leads to the creation of several disordered polymeric phases, the so-called ultrahard fullerite phases [8, 9]. The detailed X-ray studies of these phases have revealed their 3D polymeric character [10, 11].

The polymerization of C₆₀ is characterized by the destruction of a number of double C=C intramolecular bonds and the creation of intermolecular covalent bonds associated with *sp*³-like fourfold coordinated carbon atoms in the fullerene molecular cage. Their number increases from 4 to 8 and to 12 per each cage for 1D(O), 2D(T), and 2D(R) polymeric phases, respectively, and is expected to further increase in the 3D polymeric phases. Theoretical studies by Okada *et al.* [12] have predicted that the 3D-polymerized C₆₀ might be formed by the application of uniaxial pressure perpendicular to the polymeric sheets of the 2D(T) phase of C₆₀. According to their density-functional calculations, polymerization occurs at the lattice constant *c* = 10.7 Å, which is attainable at the pressure of approximately 20.2 GPa. This polymerization results in the formation of a stable metallic phase having 24 *sp*³-like and 36 *sp*²-like hybridized carbon atoms in each C₆₀ molecule. Another theoretical study, by Burgos *et al.* [13],

[¶]This article was submitted by the authors in English.

predicted that uniaxial compression perpendicular to the chains in the 1D or to the polymeric planes in the 2D polymeric phases of C_{60} leads to 3D polymerization with 52, 56, and even 60 sp^3 -like coordinated carbon atoms per C_{60}

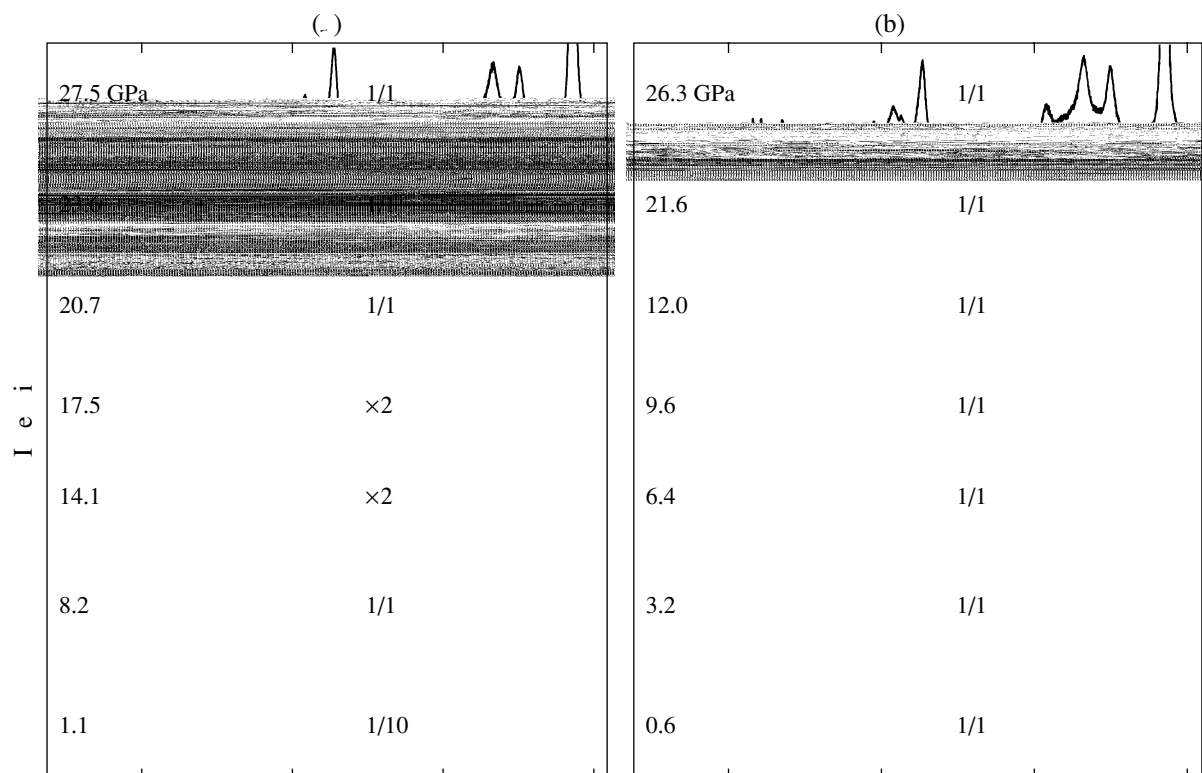


Fig. 1. Raman spectra of the $2D(T)$ polymer of C_{60} at 300 K and various pressures, recorded for (a) increasing and (b) decreasing pressure runs. The numbers $1/x$ indicate the relative scale of the spectra.

mond appearing at 1332 cm^{-1} at ambient pressure [28] is omitted. The initial spectrum at 1.1 GPa represents a typical Raman spectrum of the $2D(T)$ polymeric phase and is identical with the spectra reported earlier [14, 17, 18]. Lowering the molecular symmetry from I_h in pristine C_{60} to D_{2h} in the $2D(T)$ polymer results in the splitting of the degenerate icosahedral intramolecular modes and in the activation of initially silent modes [14, 29, 30]. Moreover, although the $2D(T)$ phase retains the inversion center of the pristine C_{60} molecule, we cannot discard the possibility that imperfections in the crystal structure of the polymer and/or the natural ^{13}C substitution may facilitate the appearance of some ungerade modes in its Raman spectrum [30]. For these reasons, the Raman spectrum of the $2D(T)$ polymer is richer in structure than that of pristine C_{60} [31].

As can be clearly seen from Fig. 1a, the Raman peaks of the $2D(T)$ polymer remain narrow and well resolved for pressures up to 14 GPa, showing the homogeneity and stability of the samples used. We note that, as recently shown [30], the pressure behavior of the Raman modes of the $2D(T)$ polymer is fully reversible up to 12 GPa. For pressures $P > 14$ GPa, the Raman peak bandwidths of the polymer increase gradually and the intensities of peaks decrease considerably. In addition, the peak broadening is accompanied by a gradual enhancement of the background (not shown in Fig. 1,

because the Raman spectra are presented after the background subtraction). As the fluorescence from the $2D(T)$ polymer of C_{60} appears in another energy region, this background is most probably related to the enhancement of strain and inhomogeneity within the sample induced at higher pressure.

The drastic changes in the Raman spectrum of the $2D(T)$ polymer are first observed at $P > 20$ GPa, where new distinct peaks appear in the spectrum and their intensities increase with a further increase in pressure. On the contrary, some of the initial Raman peaks of the polymer disappear above this critical pressure. At $P \geq 20$ GPa, the Raman spectrum of the material is significantly different from the initial one at lower pressure; the observed changes can be attributed to the transition of the polymer to a new high-pressure phase. From Fig. 1a, it is clear that, even for an applied pressure as high as 27.5 GPa, the Raman spectrum of the high-pressure phase is well resolved with relatively narrow peaks. Moreover, the frequency positions of the majority of the peaks in the new phase can be tracked back to the peaks observed in the initial $2D(T)$ polymeric phase of C_{60} . This is a first experimental indication that the C_{60} molecular cages are retained at pressures higher than 20 GPa, as the Raman peaks in the high-pressure phase have their origin on intramolecular cage vibrations.

Figure 1b shows the Raman spectra of the material upon pressure release. The decrease in pressure from 27.5 GPa to ambient conditions results in the gradual shift of the Raman peaks to lower energies. The release of pressure does not lead to any observable changes in

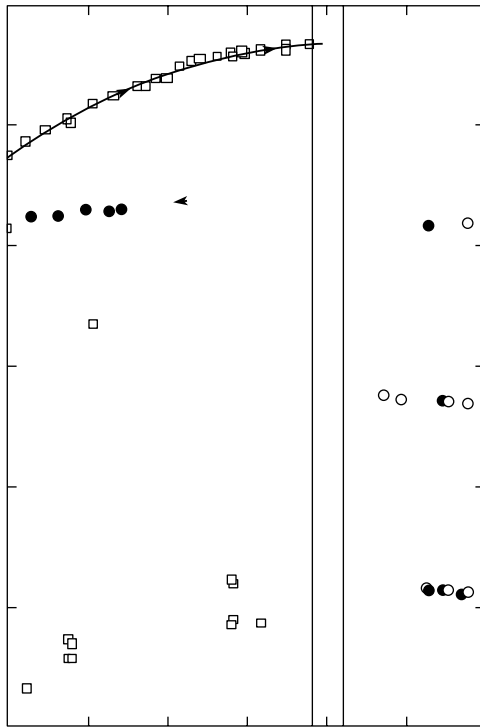
Phonon frequencies, pressure coefficients, and the Grüneisen parameters for the initial 2D(T) polymeric phase of C₆₀, the high-pressure phase, and pristine C₆₀. The phonon frequencies for the diamond-like carbon and dimeric C₆₀ phases observed after the sample detonation are also included

Mode ^a	2D(T) polymeric C ₆₀			High-pressure phase			Pristine C ₆₀			Dimer C ₆₀	Diamond-like phase	
	ω_i , cm ⁻¹	$\partial\omega_i/\partial P$, cm ⁻¹ GPa ^b	γ_i	ω_i , cm ⁻¹	$\partial\omega_i/\partial P$, cm ⁻¹ GPa ^b		γ_i	ω_i , cm ⁻¹	$\partial\omega_i/\partial P$, cm ⁻¹ GPa ^b	γ_i	ω_i , cm ⁻¹	ω_i , cm ⁻¹
		$P < 4$ GPa			$P < 10$ GPa	$P > 10$ GPa		$0.4 \text{ GPa} < P < 2.4 \text{ GPa}$				
$H_g(1)$	259	5.8	0.78	–	–	–	–	272	3.2	0.165	266	–
$H_g(1)$	282	2.3	0.264	297	0.3	0.047	0.047	294	2.5	0.119	–	–
$F_{2u}(1)$	363	–0.2	–0.019	391	–0.2	–0.024	–0.024	345	2.9	0.118	–	–
$H_g(2)$	416	–0.1	–0.009	–	–	–	–	389	–0.2	–0.007	–	–
$H_g(2)$	432	0.6	0.049	442	0.6	0.064	0.064	435	2.4	0.077	427	–
$H_g(2)$	456	0.3	0.023	459	0.8	0.079	0.079	454	1.4	0.043	–	–
$A_g(1)$	487	4.5	0.322	–	–	–	–	495	4.2	0.119	489	–
$F_{1u}(1)$	–	–	–	–	–	–	–	522	1.4	0.027	523	–
$F_{2g}(1)$	536	1.4	0.091	540	0.6	0.052	0.052	–	–	–	–	–
$F_{1g}(1)$	563	1.4	0.087	554	1.3	0.8	0.111	563	0.8	0.02	–	–
$F_{1g}(1)$	588	0.8	0.047	571	1.8	0.9	0.148	–	–	–	–	–
–	–	–	–	634	2.7	0.9	0.201	624	1.5	0.034	–	–
$H_g(3)$	666	0.7	0.036	–	–	–	–	–	–	–	–	–
$H_g(3)$	683	2.3	0.118	688	1.4	1.0	0.096	–	–	–	–	–
$H_g(3)$	–	–	–	–	–	–	–	710	–0.8	–0.016	704	–
$H_g(4)$	748	–0.7	–0.033	738	1.9	1.3	0.121	729	–2.9	–0.056	–	–
$H_g(4)$	751 ^c	–	–	–	–	–	–	755	–4.1	–0.078	–	–
$H_g(4)$	772	–1.2	–0.054	769	2.1	1.6	0.128	772	–2.7	–0.049	768	–
$H_g(4)$	773 ^c	–	–	–	–	–	–	–	–	–	–	–
–	–	–	–	826	2.4	0.137	0.137	–	–	–	–	–
$H_u(4)$	861	–0.6	–0.024	877	1.6	0.086	0.086	–	–	–	847	841
–	–	–	–	902	2.1	0.109	0.109	–	–	–	–	–
–	–	–	–	915	2.2	0.113	0.113	–	–	–	–	915
$G_g(2)$	955	4.5	0.164	961	3.0	0.147	0.147	–	–	–	956	–
–	–	–	–	972	3.7	0.179	0.179	–	–	–	–	–
$F_{2u}(4)$	1041	4.2	0.141	1029	3.8	0.174	0.174	–	–	–	–	–
–	–	–	–	1064	2.8	0.124	0.124	–	–	–	–	–
$H_g(5)$	1107	4.8	0.151	–	–	–	–	–	–	–	–	–
$G_g(3)$	1178	6.7	0.198	–	–	–	–	–	–	–	–	–
$F_{2g}(3)$	1206	7.6	0.22	–	–	–	–	–	–	–	–	–
$H_g(6)$	–	–	–	–	–	–	–	–	–	–	1239	–
$F_{2u}(5)$	–	–	–	–	–	–	–	–	–	–	1328	D1342
$H_g(7)$	1403	6.6	0.164	–	–	–	–	1422	9.8	0.096	1420	–
$A_g(2)$	1448	6.1	0.147	1430	4.3	0.14	0.14	1467	5.5	0.053	1461	–
$F_{1g}(3)$	1464	7.6	0.181	–	–	–	–	–	–	–	–	–
$F_{2g}(4)$	1541	5.1	0.115	1509	3.9	0.119	0.119	–	–	–	–	–
$H_g(8)$	1572	5.9	0.131	1567	3.7	0.111	0.111	1570	4.8	0.043	1566	G1591
$G_g(6)$	1623	4.7	0.1	1647	4.1	0.117	0.117	–	–	–	1624	–
–	–	–	–	1842	3.5	0.089	0.089	–	–	–	–	–

^a The mode assignment refers to the irreducible representations of the icosahedral C₆₀ molecule [40] and follows that in [14]; it is given here only for the initial phase of the 2D(T) polymer and the “dimeric” C₆₀ phase.

^b Data taken from [30].

^c Frequency value at $P = 6$ GPa.



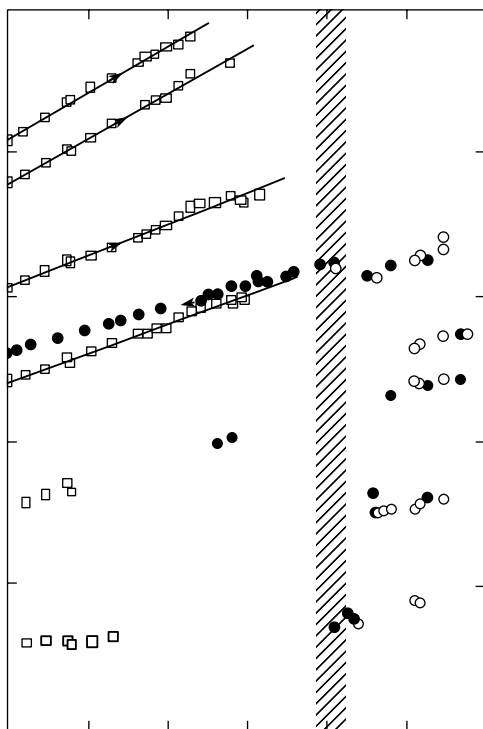
minority among the pieces of the detonated sample as the diamond-like phase, and we ascribe the respective Raman peaks of this phase at 1342 cm^{-1} and 1591 cm^{-1} (Fig. 2d, table) to the *D* (diamond) and the *G* (graphite) peak of the microcrystalline graphite [38].

The obtained experimental data provide a strong indication that the *2D(T)* polymer of C_{60} undergoes a phase transition above 20 GPa. The transformation occurs via an intermediate state having a rather diffuse Raman spectrum, which characterizes a highly disordered pretransitional state of the material at a pressure near 4 GPa. The fact that the prominent Raman peaks of the high-pressure phase are related to the retention of the C_{60} cages in this phase is an indication that the new phase of the polymer may be related to a three-dimensional (*3D*) polymerization of C_{60} . The observed peculiarities in the pretransitional pressure range also support the assumption of a further pressure-induced polymerization, which is a solid-state chemical reaction rather than a structural phase transformation. The Raman spectrum of the high-pressure phase is dominated by a very strong Raman peak around 1842 cm^{-1} , which cannot be related to any internal vibrational mode of the C_{60} molecular cage. The strong Raman

peaks ranged near $1600\text{--}1900\text{ cm}^{-1}$ in some chemical compounds of carbon are related to the stretching vibrations of isolated double $\text{C}=\text{C}$ bonds [39]. In analogy to that, the strong peak at 1842 cm^{-1} can be attributed to the destruction of a number of double $\text{C}=\text{C}$ bonds during further polymerization of the *2D(T)* polymer and to the appearance of some of the remaining ones as isolated $\text{C}=\text{C}$ bonds in the *3D* network of the C_{60} polymeric material. A more detailed analysis of the phonon modes and their pressure behavior in the initial *2D(T)* polymer and in the high-pressure phase are discussed in the next subsection.

3.2. Phonon Modes

The pressure dependence of the Raman modes of the *2D(T)* polymer of C_{60} in the initial phase (squares) and the high-pressure phase (circles) is shown in Figs. 3 and 4. The open (solid) symbols denote data taken for increasing (decreasing) pressure runs. Solid lines are drawn to guide the eye, and arrows indicate the pressure increase or decrease. In these figures, the mode assignment refers to the irreducible representations of the parent C_{60} molecule (I_h symmetry) [40], fol-



lowing the same notation as in [14] in general, and is given here only for the initial $2D(T)$ phase of the polymer. The table contains a compilation of the mode assignment (given for the initial $2D(T)$ polymeric and the “dimeric” C_{60} phases), phonon frequencies ω_i , pressure coefficients $\partial\omega_i/\partial P$, and the corresponding Grüneisen parameters γ_i that in the present work are defined for the initial $2D(T)$ polymeric and high-pressure phases. The Grüneisen parameters

$$\gamma_i = -\frac{\partial\omega_i/\omega_i}{\partial V/V} = \frac{B_0 \partial\omega_i}{\omega_i^0 \partial P}$$

have been calculated using the experimental data of the pressure coefficients $\partial\omega_i/\partial P$ for the phonon modes in both phases of the $2D(T)$ polymer. The bulk modulus $B_0 = 34.8$ GPa for the initial $2D(T)$ polymeric phase was taken from [19]. Because of the absence of any experimental data for this material, we have also used the theoretical value of the bulk modulus $B_0 = 47$ GPa [12] for the calculations of the Grüneisen parameters in the high-pressure phase. We note that the values of γ_i for the high-pressure phase are only an estimate because the real value of B_0 can differ from the theoretically predicted one. The appropriate data of the phonon mode frequencies of pristine C_{60} and their pressure coefficients and Grüneisen parameters calculated using the bulk modulus $B_0 = 14.4$ GPa [41] are included

in the table for comparison [42]. The last two columns in the table contain the phonon mode frequencies for the two phases (diamond-like and dimeric C_{60}) observed after the sample detonation at ambient conditions.

As can be seen from Figs. 3 and 4, all the Raman peaks of the initial $2D(T)$ phase disappear in the pressure range $16 \text{ GPa} < P < 20 \text{ GPa}$, while the Raman peaks related to the high-pressure phase gradually appear and gain in intensity above 20 GPa (the shaded area in Figs. 3 and 4 indicates the pressure range of the transformation). It is also clear that the majority of the Raman modes of the high-pressure phase are related to those of the $2D(T)$ polymer, showing that they originate from the C_{60} molecular cage vibrations. The nature of some phonon modes in the initial phase of the $2D(T)$ polymer of C_{60} , in particular, the Raman peak near 1040 cm^{-1} , is related to the covalent intermolecular bonding within the $2D$ polymeric layers [1, 14, 21]. More specifically, the peak near 1040 cm^{-1} is associated with the vibrations of the sp^3 -like coordinated carbon atoms; the much lower frequency of this peak compared to that of the T_{2g} mode of diamond [28] can be attributed to the different lengths of the sp^3 -like bonds in the $2D(T)$ polymer (1.64 \AA) and diamond (1.54 \AA). In the recovered high-pressure phase, this mode appears to have two components with the frequencies

1029 and 1064 cm^{-1} . Assuming that the high-pressure phase is related to the formation of a 3D polymeric phase of C_{60} proposed by Okada *et al.* [12], we can associate these two Raman peaks with the existence of two types of sp^3 -like coordinated carbon atoms with slightly different bond lengths.

Another important feature in the phonon spectrum of the high-pressure phase is the drastic changes in the region of the $A_g(2)$ pentagonal-pinch (PP) mode with respect to pristine C_{60} and its 2D(T) polymeric phase. The PP mode in pristine C_{60} is related to the in-phase stretching vibration of the five double C=C bonds orig-

4. CONCLUSIONS

The Raman scattering data under high hydrostatic pressure show that an irreversible transformation occurs in the $2D(T)$ polymeric phase of C_{60} above 20 GPa. The new phase is preceded by a pretransitional state characterized by diffuse Raman peaks. The spectrum of the high-pressure phase remains intense and well resolved at pressures as high as 30 GPa. The phonon modes of the high-pressure phase, especially in the high-energy region, are noticeably different from those of the initial $2D(T)$ polymer; nevertheless, they can be tracked back to the phonon modes related to the fullerene molecular cage. The recovered high-pressure phase is metastable and detonates under laser irradiation. The main part of the detonated sample is a mixture of monomeric and dimeric C_{60} , showing that the fullerene molecular cages are retained in the high-pressure phase. The high-pressure phase seems to be related to further creation of covalent bonds between molecules belonging to the adjacent polymeric layers in accordance with the theoretically predicted $3D$ polymerization of the $2D(T)$ C_{60} polymer at 20.2 GPa [12]. Our Raman experiments reveal that the $3D$ polymeric C_{60} resulting from the application of high pressure on the $2D(T)$ polymer is not related to the earlier observed ultrahard fullerite phases [1, 8, 9]. The electronic spectrum of the $2D(T)$ polymer is noticeably different from that of the pristine C_{60} . This difference is related both to the deformation of the fullerene molecular cage caused by the polymerization of material and to the decrease in the in-plane intermolecular distances in the $2D(T)$ polymer.

ACKNOWLEDGMENTS

The support by the General Secretariat for Research and Technology, Greece, is gratefully acknowledged. One of the authors (K.P.M.) acknowledges the support by the Russian State Research Program "Physical Properties of Carbon-Based Nanostructures and Development of New Electronic Devices." Another (B.S.) acknowledges the support from the Swedish Research Councils for Natural Sciences (NFR) and Engineering Sciences (TFR).

The authors thank A. Soldatov and T. Wägberg for help with preparation and characterization of the $2D(T)$ polymer of C_{60} .

REFERENCES

1. B. Sundqvist, *Adv. Phys.* **48**, 1 (1999).
2. A. M. Rao, P. Zhou, K.-A. Wang, *et al.*, *Science* **259**, 955 (1993).
3. P. W. Stephens, G. Bortel, G. Faigel, *et al.*, *Nature (London)* **370**, 636 (1994).
4. K. Prassides, K. Vavakis, K. Kordatos, *et al.*, *J. Am. Chem. Soc.* **119**, 834 (1997).
5. Y. Iwasa, T. Arima, R. M. Fleming, *et al.*, *Science* **264**, 1570 (1994).
6. M. Nunez-Regueiro, L. Marques, J.-L. Hodeau, *et al.*, *Phys. Rev. Lett.* **74**, 278 (1995).
7. V. V. Brazhkin, A. G. Lyapin, and S. V. Popova, *Pis'ma Zh. Éksp. Teor. Fiz.* **64**, 755 (1996) [*JETP Lett.* **64**, 802 (1996)].
8. V. D. Blank, M. Yu. Popov, S. G. Buga, *et al.*, *Phys. Lett. A* **188**, 281 (1994).
9. V. D. Blank, S. G. Buga, G. A. Dubitsky, *et al.*, *Carbon* **36**, 319 (1998).
10. L. Marques, M. Mezouar, J.-L. Hodeau, *et al.*, *Science* **283**, 1720 (1999).
11. L. A. Chernozatonskii, N. R. Serebryanaya, and B. N. Mavrin, *Chem. Phys. Lett.* **316**, 199 (2000).
12. S. Okada, S. Saito, and A. Oshiyama, *Phys. Rev. Lett.* **83**, 1986 (1999).
13. E. Burgos, E. Halac, R. Weht, *et al.*, *Phys. Rev. Lett.* **85**, 2328 (2000).
14. V. A. Davydov, L. S. Kashevarova, A. V. Rakhmanina, *et al.*, *Phys. Rev. B* **61**, 11936 (2000).
15. G. A. Kourouklis, S. Ves, and K. P. Meletov, *Physica B (Amsterdam)* **265**, 214 (1999).
16. J. Arvanitidis, K. Papagelis, I. Tsilika, *et al.*, *Physica B (Amsterdam)* **265**, 234 (1999).
17. K. P. Meletov, J. Arvanitidis, I. Tsilika, *et al.*, *Phys. Rev. B* **63**, 054106 (2001).
18. K. P. Meletov, S. Assimopoulos, I. Tsilika, *et al.*, *Chem. Phys. Lett.* **341**, 435 (2001).
19. J. M. Leger, J. Haines, V. A. Davydov and V. Agafonov, *Solid State Commun.* **121**, 241 (2002).
20. K. P. Meletov, J. Arvanitidis, G. A. Kourouklis, *et al.*, submitted to *Chem. Phys. Lett.* (2002).
21. T. Wegberg, A. Soldatov, and B. Sundqvist, unpublished.
22. R. Moret, P. Launois, T. Wägberg, *et al.*, *Eur. J. Phys. B* **15**, 253 (2000).
23. K. P. Meletov, E. Liarokapis, J. Arvanitidis, *et al.*, *Chem. Phys. Lett.* **290**, 125 (1998).
24. P.-A. Persson, P. Jacobsson, S. Stafstrom, *et al.*, *Europhys. Lett.* **49**, 631 (2000).
25. P.-A. Persson, U. Edlund, P. Jacobsson, *et al.*, *Chem. Phys. Lett.* **258**, 540 (1996).
26. A. Jayaraman, *Rev. Sci. Instrum.* **57**, 1013 (1986).
27. D. Barnett, S. Block, and G. J. Piermarini, *Rev. Sci. Instrum.* **44**, 1 (1973).
28. S. A. Solin and A. K. Ramdas, *Phys. Rev. B* **1**, 1687 (1970).
29. V. A. Davydov, L. S. Kashevarova, A. V. Rakhmanina, *et al.*, *Phys. Rev. B* **58**, 14786 (1998).
30. J. Arvanitidis, K. P. Meletov, K. Papagelis, *et al.*, *J. Chem. Phys.* **114**, 9099 (2001).
31. K. P. Meletov, D. Christofflos, S. Ves, *et al.*, *Phys. Rev. B* **52**, 10090 (1995).
32. V. V. Brazhkin, A. G. Lyapin, S. V. Popova, *et al.*, *Phys. Rev. B* **56**, 11465 (1997).
33. V. D. Blank, S. G. Buga, N. R. Serebryanaya, *et al.*, *Carbon* **36**, 665 (1998).
34. V. V. Brazhkin, A. G. Lyapin, S. V. Popova, *et al.*, *J. Appl. Phys.* **84**, 219 (1998).

35. M. Weiler, S. Sattel, T. Giessen, *et al.*, Phys. Rev. B **53**, 1594 (1996).
36. R. J. Nemanich and S. A. Solin, Phys. Rev. B **20**, 392 (1979).
37. R. E. Shroder, R. J. Nemanich, and J. T. Glass, Phys. Rev. B **41**, 3738 (1990).
38. M. S. Dresselhaus, M. A. Pimenta, P. C. Eklund, *et al.*, in *Raman Scattering in Material Science*, Ed. by W. H. Weber and R. Merlin (Springer-Verlag, Berlin, 2000), p. 314.
39. D. A. Long, *Raman Spectroscopy* (McGraw-Hill, London, 1976), p. 158.
40. M. C. Martin, X. Du, J. Kwon, and L. Mihaly, Phys. Rev. B **50**, 173 (1994).
41. J. Haines and J. M. Leger, Solid State Commun. **90**, 361 (1994).
42. K. P. Meletov, G. Kourouklis, D. Christofflos, *et al.*, Zh. Éksp. Teor. Fiz. **108**, 1456 (1995) [JETP **81**, 798 (1995)].
43. A. F. Goncharov, I. N. Makarenko, and S. M. Stishov, Pis'ma Zh. Éksp. Teor. Fiz. **41**, 150 (1985) [JETP Lett. **41**, 184 (1985)].
44. K. P. Meletov and V. D. Negrii, Pis'ma Zh. Éksp. Teor. Fiz. **68**, 234 (1998) [JETP Lett. **68**, 248 (1998)].
45. F. Negri, G. Orlandi, and F. Zerbetto, Chem. Phys. Lett. **144**, 31 (1988).
46. F. Negri, G. Orlandi, and F. Zerbetto, J. Chem. Phys. **97**, 6496 (1992).
47. G. Herzberg and E. Teller, Z. Phys. Chem., Abt. B **21**, 410 (1933).
48. W. Guss, J. Feldman, E. O. Gobel, *et al.*, Phys. Rev. Lett. **72**, 2644 (1994).
49. K. P. Meletov, S. Assimopoulos, and G. A. Kourouklis, unpublished.

SPELL: dime[←]